A Model for the Pion Structure Function

F. Bissey, J. R. Cudell, J. Cugnon, M. Jaminon,
J. P. Lansberg and P. Stassart

Université de Liège, Département de Physique B5, Sart Tilman,
B-4000 LIEGE 1, Belgium

Abstract

The pion structure function is investigated in a simple model, where pion and constituent quark fields are coupled through the simplest pseudoscalar coupling. The imaginary part of the forward $\gamma^\star\pi \to \gamma^\star\pi$ scattering amplitude is evaluated and related to the structure functions. It is shown that the introduction of non-perturbative effects, linked to the size of the pion and preserving gauge invariance, allows a connection with the quark distribution. It is predicted that higher-twist terms become negligible for Q^2 larger than $\sim$2 GeV^2 and that quarks in the pion have a momentum fraction smaller than in the proton case.

Key words: Pion structure function, Gauge invariance, Non-perturbative effects
PACS: 13.60.Hb, 13.60.Fz, 14.40.Aq, 12.38.Aw

1 Introduction

Deep-inelastic scattering (DIS) experiments provide us with a wealth of information about the structure of hadrons, usually cast in the form of structure functions. These data are only partly understood in the framework of quantum chromodynamics (QCD). Indeed, perturbative QCD is consistent with the Q^2 evolution of the structure functions at sufficiently high Q^2 and x [1]. However, it is neither able to predict the structure functions themselves, as the latter are supposed to result from non-perturbative effects, among which confinement and spontaneous chiral symmetry breaking, nor the magnitude of the initial value Q_0^2 from which the Q^2 dependence can be evaluated . The interest has recently widened to off-diagonal parton distributions [2–5], which potentially offer to reach complementary information, especially about parton correlations.

Phenomenological quark models, which possess some non-perturbative aspects and which are rather successful in reproducing low-energy properties

of hadrons, are expected to help us to understand the connection between DIS data and non-pertubative aspects. Pions and other low-mass mesons are the simplest systems for which effective models exist that incorporate, in some simplified way, such special QCD features such as spontaneous chiral symmetry breaking and anomalies.

Our original plan was to investigate the properties of off-diagonal parton distributions in a simple model for light mesons. However, we realized that the theoretical investigation of the diagonal distributions using phenomenological quark models is far from being settled. There have been several theoretical investigations along these lines in recent years [6–9]. They rely on the assumption that distributions evaluated in leading-twist approximation at small Q^2, where these models apply, can serve as input in the DGLAP evolution equations [10] to generate parton distributions that are directly comparable with experimental data at large Q^2 [11–15]. This is a rather tricky point as it is not clear that a good approximation at low Q^2 can be evolved by perturbative equations to large Q^2, as it is not sure that, in this regime, the forward $\gamma^\star\pi \to \gamma^\star\pi$ amplitude can be parametrised in terms of parton distributions (despite the existence of low-Q^2 parametrisations [14,15]).

Some of the theoretical works mentioned above have been carried out in the framework of the Nambu and Jona-Lasinio (NJL) model [16]. This model is indeed quite successful in reproducing low-energy phenomenology and embodies chiral symmetry breaking, which is believed to be crucial for this success. However, investigations of the structure functions have given rather different results [7–9]. This situation originates from the fact that the NJL model needs to be regularized and that different regularizations yield different results.

We show in this paper that these complications may in fact be avoided. We investigate the simplest model of a pion, in which the $q\overline{q}\pi$ vertex is represented by the simplest pseudoscalar coupling. Of course, the quark fields and the coupling constant should reflect in some way the properties of actual pions. One possible guide is provided by the large N_c limit of the NJL model. The latter is equivalent, in the chirally broken phase, to a σ-model with massive constituent quarks and an effective pion-quark-quark coupling constant. Our starting point for the investigation of the parton distributions of the pion consists in a Lagrangian that includes massive pion and massive quark fields interacting through the simplest pseudoscalar vertex. We show below that there is no need to regularize this model as the imaginary part of the forward $\gamma^\star\pi \to \gamma^\star\pi$ scattering amplitude is finite. However, the interaction between the constituent quarks should vanish when their relative momentum is large enough. It is possible to cope with this requirement by imposing a finite momentum cut-off, which mimics the effect of a pion wave function. Such a step leads to the appearance of a straightforward relation between the $\gamma^\star - \pi$ cross sections and the quark distributions at high enough Q^2, as we shall show

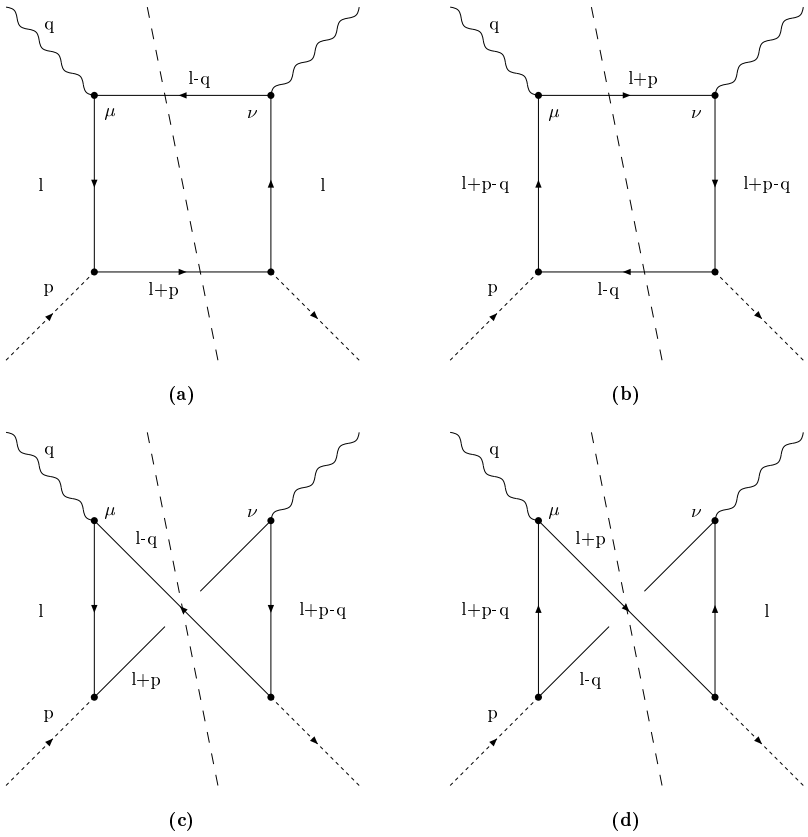

Fig. 1. Simplest diagrams contributing to the imaginary part of the forward amplitude for the scattering of a virtual photon by a neutral pion. Upper (lower) diagrams are referred to as box (crossed) diagrams. Dashed lines represent the discontinuity of the amplitudes or their imaginary parts.

below.

2 The model

We consider an isospin triplet pion field $\vec{\pi} = (\pi^+, \pi^0, \pi^-)$ interacting with quark fields ψ through the Lagrangian density

$$\mathcal{L}_{int} = ig(\overline{\psi}\ \vec{\tau}\gamma_5\psi).\ \vec{\pi}, \tag{1}$$

where $\vec{\tau}$ is the isospin vector operator. It is our purpose to calculate the imaginary part of the forward elastic $\gamma^\star - \pi$ scattering amplitude, or equivalently the total cross-section, in the simplest approximation and extract from it the pion structure functions W_1 and W_2. Finally, we want to see whether they are reducible to quark distributions. We give below explicit results for the neutral pion.

The relevant diagrams contributing to the imaginary part of the forward elastic scattering amplitude, up to first order in α, the fine structure constant, and to second order in g, are given in Fig. 1. We define the pion 4-momentum as p, the photon 4-momentum as q, the (u and d) quark constituent mass as m_q and we use $p^2 = m_\pi^2$, $q^2 = -Q^2$, $p.q = \nu$, $x = Q^2/(2\nu)$. This leads to $s = m_\pi^2 + Q^2(1/x - 1)$. The imaginary part of the amplitudes can be written, using Cutkosky rules, as

$$\mathrm{Im}T^a_{\mu\nu} = -2Cg^2 \int d^4l \{t^1_{\mu\nu} D_1 D_4 D_1 D_2\}, \tag{2}$$

$$\mathrm{Im}T^c_{\mu\nu} = -2Cg^2 \int d^4l \{t^2_{\mu\nu} D_1 D_4 D_3 D_2\}, \tag{3}$$

with the fermionic traces

$$\begin{aligned} t^1_{\mu\nu} = & \mathrm{Tr}\left[\gamma_\mu(\gamma.(l-q) + m_q)\gamma_\nu \right. \\ & \left. (\gamma.l + m_q)\gamma_5(\gamma.(l+p) + m_q)\gamma_5(\gamma.l + m_q)\right], \end{aligned} \tag{4}$$

$$\begin{aligned} t^2_{\mu\nu} = & \mathrm{Tr}\left[\gamma_\mu(\gamma.(l-q) + m_q)\gamma_5(\gamma.(l+p-q) + m_q)\gamma_\nu \right. \\ & \left. (\gamma.(l+p) + m_q)\gamma_5(\gamma.l + m_q)\right], \end{aligned} \tag{5}$$

and the fermion propagators (or their contribution to the cuts)

$$\begin{aligned} D_1^{-1} &= l^2 - m_q^2, & D_2 &= 2\pi\delta\left((l+p)^2 - m_q^2\right), \\ D_3^{-1} &= (l+p-q)^2 - m_q^2, & D_4 &= 2\pi\delta\left((l-q)^2 - m_q^2\right). \end{aligned} \tag{6}$$

The constant $C = 5e^2/(384\pi^6)$ accounts for flavour, charge and loop momentum integration factors in the particular case (neutral pion) under consideration. Diagrams (b) and (d) have the same contributions as (a) and (c), respectively. The second ones are obtained from the first ones by the substitution $l \to q - p - l$ in the integrals. Using $T^1 = T^a + T^b$, $T^2 = T^c + T^d$ and $T = T^1 + T^2$, one can rewrite

$$\mathrm{Im}T^1_{\mu\nu} = -2Cg^2 \int d^4l \{t^1_{\mu\nu} D_1 D_4 D_1 D_2 + (l \to q - p - l)\}, \tag{7}$$

$$\mathrm{Im}T^2_{\mu\nu} = -2Cg^2 \int d^4l \{t^2_{\mu\nu} D_1 D_4 D_3 D_2 + (l \to q - p - l)\}, \tag{8}$$

which makes gauge invariance ($q^\mu \mathrm{Im}T_{\mu\nu} = \mathrm{Im}T_{\mu\nu} q^\nu = 0$) explicit by inspection of the integrand. It is worth emphasizing that the sum of the four diagrams is gauge invariant, but none of them alone has this property.

We perform the integrations in Eqs. 7 and 8 using Sudakov variables. We define $l = -\xi p + \eta q + l_t$, with l_t perpendicular to both p and q. A little algebra shows that

$$d^4l \;\; \delta((l+p)^2 - m_q^2)\delta((l-q)^2 - m_q^2) = \frac{dl^2 d\phi}{4\sqrt{\nu^2 + 2\nu m_\pi^2 x}}, \tag{9}$$

with the change of variable

$$\xi = x + \frac{(l^2 - m^2 - 2m_\pi^2)(2x-1)}{2\nu + 4m_\pi^2 x}, \tag{10}$$

and with η and l_t^2 related to l^2 through the relations

$$\eta = \frac{-l^2 + m^2 + m_\pi^2(2x-1)}{2\nu + 4m_\pi^2 x} + \frac{m_\pi^2(-l^2+m^2)}{\nu(2\nu + 4m_\pi^2 x)}, \tag{11}$$

$$\begin{aligned} l_t^2 = {} & (l^2 - m_\pi^2 x)(1-x) + m^2 x \\ & + \frac{(1-x)(-4m_\pi^2 x(l^2 - m_\pi^2 x) + (l^2 - m^2)^2)}{2\nu + 4m_\pi^2 x} \\ & + \frac{m_\pi^2(l^2 - 4m^2 x(x-1) - m^2 - m_\pi^2 x)}{2\nu + 4m_\pi^2 x} \\ & + \frac{m_\pi^2 (l^2 - m^2)^2}{4\nu^2 + 8\nu m_\pi^2 x}. \end{aligned} \tag{12}$$

The integration over the azimuthal angle ϕ is trivial and one is left only with the integration over the variable $\tau \equiv -l^2$. The integration bounds on τ come from the positivity of the energies of the on-shell intermediate states (see Fig. 1) and from the space-like definition of l_t (yielding $l_{t0}^2 \leq 0$), which introduces the most stringent constraints. The latter take the following forms:

$$\begin{aligned} \tau \leq 2\nu + {} & \frac{((1-x)x m_\pi^2 - (2-x)m_q^2)}{1-x} \\ & - \frac{(m_q^2 - x^2 m_\pi^2)(m_q^2 - (1-x)^2 m_\pi^2)}{2\nu(1-x)^2}, \end{aligned} \tag{13}$$

and

$$\tau \geq \frac{(m_q^2 - (1-x)m_\pi^2)}{1-x} + \frac{(m_q^2 - x^2 m_\pi^2)(m_q^2 - (1-x)^2 m_\pi^2)}{2\nu(1-x)^2}, \tag{14}$$

where only the first terms in the expansion of the r.h.s. in $1/\nu$ are given (the full expressions are used in numerical evaluations).

The structure functions W_1 and W_2 being defined by

$$\begin{aligned} W_{\mu\nu} &= \frac{1}{2\pi}\mathrm{Im}T_{\mu\nu} \\ &= \left(-g_{\mu\nu} + \frac{q_\mu q_\nu}{q^2}\right) W_1 + \left(p_\mu - q_\mu \frac{p.q}{q^2}\right)\left(p_\nu - q_\nu \frac{p.q}{q^2}\right) W_2, \end{aligned} \tag{15}$$

they can be calculated through the contractions

$$W^\mu_\mu = \frac{-6xW_1 + (\nu + 2m_\pi^2 x)W_2}{2x}, \tag{16}$$

$$p^\mu p^\nu W_{\mu\nu} = \frac{-2x(\nu + 2m_\pi^2 x)W_1 + (\nu + 2m_\pi^2 x)^2 W_2}{4x^2}. \tag{17}$$

We also checked that we get the same results for W_1 and W_2 by computing directly the $\gamma^\star\pi \to q\overline{q}$ transverse and longitudinal cross-sections.

Although we give below results for the exact expressions, it is worth giving the large-Q^2 limit:

$$W_1 = \frac{5g^2}{24\pi^2}\left[\ln\left(\frac{2(1-x)\nu}{M^2}\right) - \frac{m_\pi^2}{M^2}x(1-x)\right], \tag{18}$$

with $M^2 = m_q^2 - m_\pi^2 x(1-x)$.

At this point, the pion cannot be interpreted as a collection of partons with a probability distribution. Indeed, the crossed diagrams are not suppressed by a power of Q^2 compared to the box diagrams and therefore do not allow such an interpretation. This is manifest when their respective contributions are written down in the combined small-m_π, large-Q^2 limit:

$$W_1^{box} = \frac{5g^2}{24\pi^2}\left[\ln\left(\frac{2(1-x)\nu}{m_q^2}\right) - 1\right], \quad W_1^{cross} = \frac{5g^2}{24\pi^2}. \tag{19}$$

A reason for the appearance of this undesirable feature is that we have not yet imposed the fact that the pion has a finite size. The simplest way to do this is to require that the square of the relative four-momentum of the quarks inside the pion is limited to a maximum value Λ^2. The former quantity is given by

$$O_1 = (p + 2l)^2 = -2\tau + 2m_q^2 - m_\pi^2, \tag{20}$$

for vertices like those in diagram Fig. 1.(a), and by

$$O_2 = (p + 2(l + p - q))^2 = 2\tau + 6m_q^2 - m_\pi^2 - 4\nu, \tag{21}$$

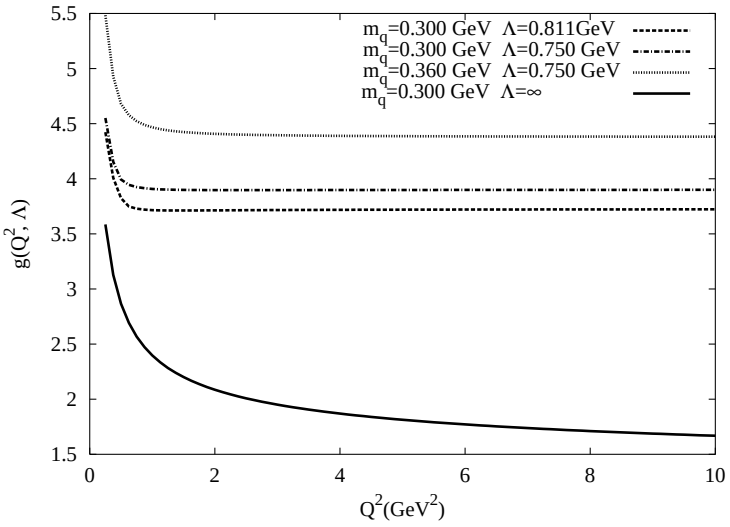

Fig. 2. Values of the coupling constant $g(Q^2, \Lambda)$ which fulfill sum rule (Eq. 25), for the values of the parameters indicated at the top.

for vertices like those in diagram Fig. 1.(b). We either require $|O_1| < \Lambda^2$ or $|O_2| < \Lambda^2$ for all diagrams, which excludes the interval $[\Lambda^2, 2\nu - \Lambda^2/2]$ from the τ integral.

$|O_1|$ and $|O_2|$ cannot be small simultaneously. The crossed diagrams have their main contribution for $O_1 \simeq O_2$, and are thus suppressed by a power Λ^2/Q^2 when the cut is imposed. The box diagrams have a leading contribution for $|O_1|$ or $|O_2|$ small, and are not power suppressed by the cut.

Physically, this happens because, for the crossed diagrams, the momentum transfer suffered by the quark (antiquark) has to be re-emitted by the antiquark (quark), which is impossible when this momentum transfer becomes too large. For the box diagrams, the transferred momentum is taken and released by the same quark (or antiquark) and there is no suppression. Note that $\tau = -t$ (for the $\gamma^\star \pi \to q\overline{q}$ process) is a physical observable quantity. This guarantees that our implementation of the cut-off is gauge-invariant. With our cut-off, the crossed diagrams appear now as higher twists: they are suppressed at least as $1/Q^2$ and the box diagram contribution can now be interpreted in terms of parton distributions. Indeed, we checked numerically that, for typical values of Λ (see Fig. 2), the ratio between the respective magnitudes of the crossed and box diagrams is roughly $\sim 0.06/Q^2$ GeV^{-2}, for x=0.1; without cut-off, this ratio is a sizable fraction of unity for Q^2 less than $\sim$ 1000 GeV^2.

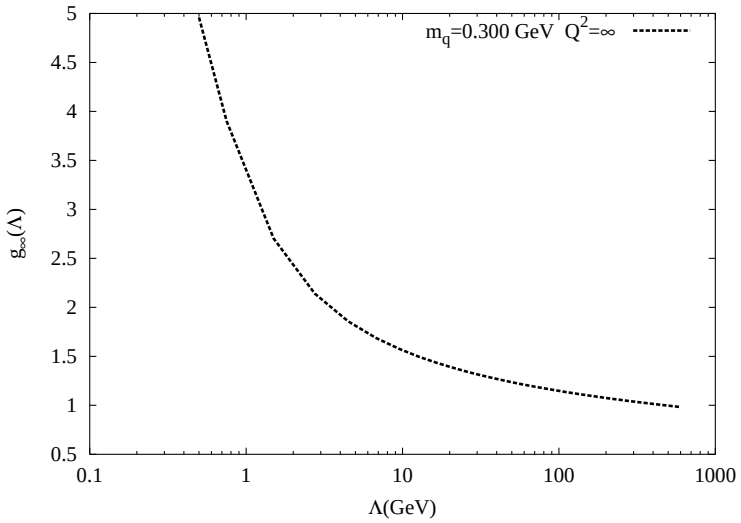

Fig. 3. Asymptotic value (for large Q^2) of the coupling constant fulfilling sum rule (Eq. 25), as a function of the cut-off parameter Λ.

3 Results

The structure functions can now be related to the (valence) quark distributions:

$$F_1 = W_1 = \frac{4}{18}(u_v(x) + \bar{u}_v(x)) + \frac{1}{18}(d_v(x) + \bar{d}_v(x)), \tag{22}$$

$$F_2 = \nu W_2 = 2xF_1. \tag{23}$$

We stress that the last relation, known as the Callan-Gross relation, comes out of our calculation. This does indicate that our approximations have been done consistently [1] .

So far, we have only described the model. In order to make predictions, we need to fix its parameters, namely Λ, m_q and g. The latter can be thought of as the normalisation of the quark wave function, and we determine it by imposing that there are only two constituent quarks in the pion. In our model, the valence quark distributions are equal

$$u_v(x) = \bar{u}_v(x) = d_v(x) = \bar{d}_v(x) \equiv v(x). \tag{24}$$

[1] For charged pions, the additional diagrams implying a direct coupling of the virtual photon to the pion are suppressed by a factor $1/s$ and the leading-twist results are the same, except for the charge coefficients entering Eq. 22.

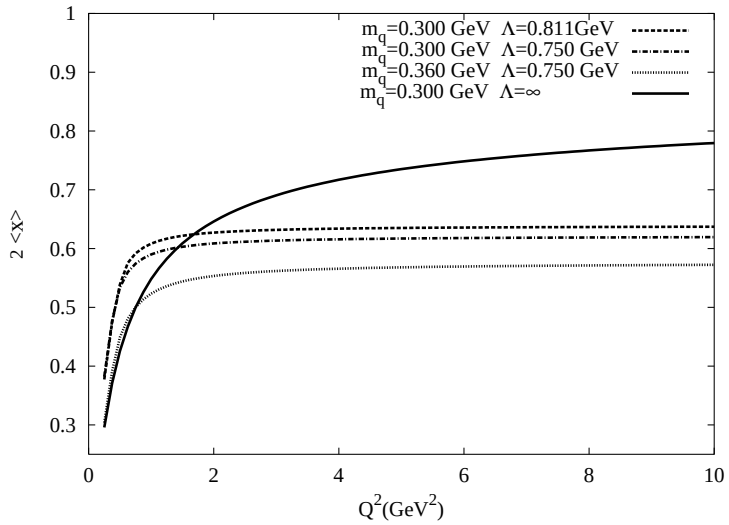

Fig. 4. Momentum fraction of the quarks inside the neutral pion (Eq. 26), as a function of Q^2, for the values of the parameters indicated at the top of the figure.

The condition $\int_0^1 v(x)dx = 1/2$ then gives us

$$\int_0^1 F_1(x)dx = \frac{5}{18}. \tag{25}$$

As F_1 is a function, not only of m_q and Λ, but also of Q^2, this gives us a coupling constant that evolves with Q^2. The resulting values of g are shown in Fig. 2: for a finite cut-off Λ, the cross-section at fixed g would grow with energy, until the pion reaches its maximum allowed size, in which case the cross section would remain constant. If we impose relation (25), this means that $g(Q^2)$ will first decrease until the cut-off makes it reach a plateau value for $Q^2 \gg \Lambda^2$ (in practice, the plateau value is reached around $Q^2 \approx 2\Lambda^2$). The plateau value depends on m_q/Λ (and m_π/Λ) and is shown in Fig. 3.

To constrain further our parameters, we can try to use the momentum sum rule

$$2\langle x\rangle = 4\int_0^1 xv(x)dx = \frac{18}{5}\int_0^1 F_2(x)dx. \tag{26}$$

In the parton model, this integral should be equal to 1 as $Q^2 \to \infty$, as we do not have gluons in the model. Indeed, there are two limits of our model that fulfill this condition automatically. First of all, if we do not impose that the pion has a finite size, then asymptotically we get $2\langle x\rangle$ =1. In the limit

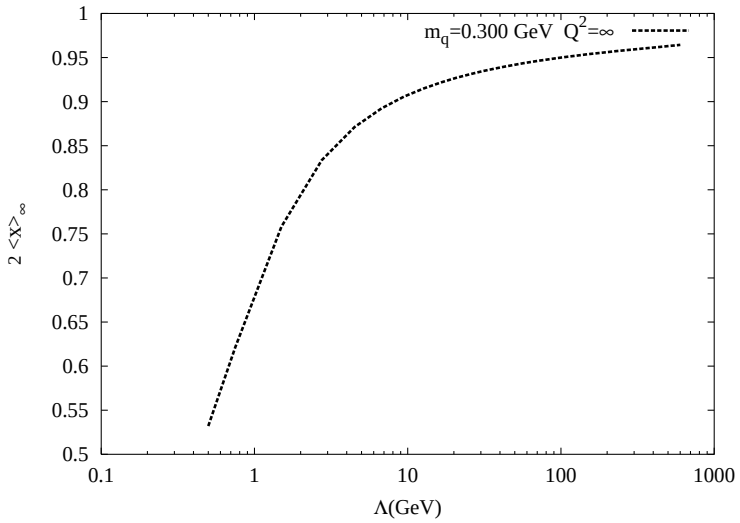

Fig. 5. Asymptotic value (for large Q^2) of the momentum fraction of the quarks inside the neutral pion (Eq. 26), as a function of the cut-off Λ.

$m_\pi = 0$, we obtain

$$2\,\langle x\rangle\,(\Lambda=\infty, m_\pi=0) = \frac{4\ln(2\nu/m_q^2)-3}{4\ln(2\nu/m_q^2)-1}. \tag{27}$$

This means that in that regime, for sufficiently high Q^2, the quarks behave as free particles, and the usual derivation based on the OPE holds [18]. The second case where this holds confirms this interpretation: if we impose $m_q \leq m_\pi/2$, the expressions we have given develop an infrared divergence, which corresponds to the case where both quarks emerging from the pion are on-shell and free. This divergence can be re-absorbed into the normalisation (25) of g, and the sum rule $2\,\langle x\rangle = 1$ is again automatically satisfied at large Q^2.

However, in the physical pion case, it makes more sense to consider that one of the quarks remains off-shell: the imposition of a cut-off changes the sum rule value, as the fields can never be considered as free. Hence, because of the Goldstone nature of the pion, one expects that the momentum sum rule will take a smaller value than in the case of other hadrons. This may explain why fits that assume the same momentum fraction for valence quarks in protons and pions [14] do not seem to leave any room for sea quarks [19]. The results for $2\,\langle x\rangle$ are shown in Fig. 4. Again, the curves show a plateau at sufficiently large Q^2, with a value depending on m_q/Λ and m_π/Λ. It is easy to show that this value is always smaller than 1. It is shown in Fig. 5 as a function of Λ.

To fix the remaining parameters, we must then use our knowledge of constituent quarks, and of the pion. We choose conservative values $m_q = 300$ MeV or 360 MeV, and a pion radius of the order of 0.25 fm, which corresponds to

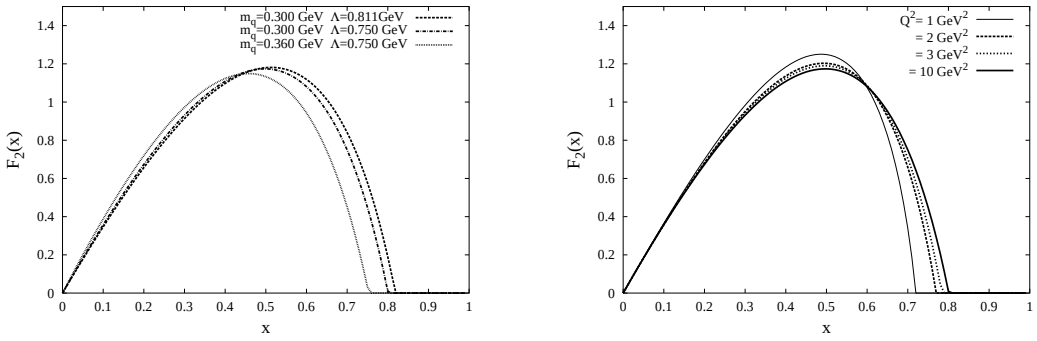

Fig. 6. Structure function F_2 for the neutral pion. On the left, Q^2=2 GeV^2 and the values of the parameters m_q and Λ are as indicated. On the right, m_q=0.3 GeV and Λ=0.75 GeV and the values of Q^2 are as indicated.

$\Lambda \simeq 800$ MeV. This choice of parameters gives us a momentum fraction $2\langle x\rangle$ between 0.55 and 0.65 (see Fig. 4), and corresponds to a coupling g with the plateau value of 3.8. It is remarkable that this value is very close to the one that guarantees in the NJL model, with the same constituent mass and the same cut-off, a unit value for the residue of the $q\overline{q}$ propagator at the pion pole and the correct value of the electric form factor at $Q^2 = 0$ [17]. In other words, this corresponds to the value needed for the pion to appear in the NJL model as constituted of a quark and an antiquark [2].

Let us finally examine the properties of the distribution $v(x)$, or equivalently, of the function F_2. Some of our results are summarized in Fig. 6, for $Q^2 = 2$ GeV^2. The most striking feature is the vanishing of this function for x larger than some value x_{max}. This is again due to the fact that, because the quarks are not free in this model, the actual value of their mass does matter. It can clearly be seen that this effect originates from kinematical cuts: in the chiral limit and for large ν, the condition $s \geq 4m_q^2$ is equivalent to $x_{max} \approx 1 - \frac{2m_q^2}{\nu}$, in the absence of cut-off.

In the case of a finite cut-off ($\Lambda^2 \ll Q^2$), conditions (13-14) lower the value of x_{max} to

$$x_{max} \approx 1 - \frac{m_q^2}{\Lambda^2}. \tag{28}$$

This means that, for a finite Q^2, when x is large, which corresponds to a small value of s, there is no way to put the cut quarks on their mass shell: this requires at least an energy of 4 m_q^2. For given Q^2 and Λ, the available energy

[2] One should note that, although the numerical values are compatible, the cut-off has different physical origins in the two approaches: it corresponds to the maximum internal momentum of the pion in our approach, while it is a parameter for regularizing ultraviolet divergences in the NJL model.

is increasing with decreasing x. As a result, putting the cut quarks on-shell will be easier for small than for large x. Therefore, the x-distribution (F_1) is expected to be enhanced on the low x side, leading to a momentum fraction smaller than unity. The vanishing at large x is not obtained in similar works, in particular in the one of Ref. [7]. In this reference, the Bjorken limit is taken first and the kinematical constraint (Eq. 13) is not applied . This procedure is certainly not correct for evaluating cross-sections at finite Q^2. Except for this vanishing, our results basically agree with those of Ref. [7]. Therefore we will not present results for the DGLAP evolution of our structure function F_2, which we expect to be compatible with the existing data.

4 Discussion and conclusion

We have discussed the simplest model allowing to relate virtual photon-pion forward elastic scattering to quark distributions. In this model, the imaginary part of the forward elastic scattering does not show any divergence. However, this quantity cannot provide the quark distributions readily since the numerical importance of the so-called crossed diagrams precludes the existence of such a relationship. The introduction of a cut-off for the relative momentum of the quarks inside the pion allows such an interpretation: crossed diagrams then appear as higher twists. The introduction of the cut-off does not allow to fulfill the momentum sum rule ($2\langle x\rangle = 1$) at infinite Q^2 because, in the case of the pion, constituent quarks can never be considered as free. We have mentioned above how the kinematical constraint, allowing quarks to be put on their mass shell, leads to the reduction of the momentum fraction. This can easily be seen from our results for the chiral limit (Eq. 27).

We motivated the cut-off as a manifestation of the pion size. The value $\Lambda^{-1} = (0.75\ \mathrm{GeV})^{-1}$ is close to the hard core rms radius of the chiral bag model, 0.35 fm [20].

The cut-off has been imposed on the relative quark momentum. This procedure is at variance with the double-subtraction Pauli-Villars procedure proposed in Ref. [9]. We have considered such a procedure in our model, but it produces discontinuities in the structure function as well as a negative value for this quantity in some regions of x. This procedure is also different from with the other ones introduced in similar works based on NJL models, where they are part of the necessary regularization of these models to avoid divergences. In addition, there is no need in our approach to consider additional diagrams with local pion-pion-quark-quark interactions. Yet, the pion-quark-quark coupling constant turns out to be the same in our approach and in NJL models. This may not be too surprising, as in both cases this coupling is determined by the requirement that the pion appears as made of two constituent quarks.

Our main conclusion is that pions are different from other hadrons, in the sense that the quark momentum fraction should be smaller, and that higher twist terms disappear for $Q^2 \sim 2$ GeV^2.

This work has been performed in the frame of the ESOP collaboration (European Union contract N° HPRN-CT-2000-00130). We thank Dr. M. Diehl and Dr. P. Guichon for their useful comments.

References

[1] A. M. Cooper-Sarkar, R. C. Devenish and A. De Roeck, Int. J. Mod. Phys. A **13** (1998) 3385 [arXiv:hep-ph/9712301].

[2] X. D. Ji, Phys. Rev. Lett. **78** (1997) 610 [arXiv:hep-ph/9603249]; Phys. Rev. D **55** (1997) 7114 [arXiv:hep-ph/9609381].

[3] A. V. Radyushkin, Phys. Lett. B **380** (1996) 417 [arXiv:hep-ph/9604317]; Phys. Rev. D **56** (1997) 5524 [arXiv:hep-ph/9704207].

[4] J. C. Collins, L. Frankfurt and M. Strikman, Phys. Rev. D **56** (1997) 2982 [arXiv:hep-ph/9611433].

[5] M. Vanderhaeghen, P. A. Guichon and M. Guidal, Phys. Rev. Lett. **80** (1998) 5064.

[6] R. L. Jaffe and G. G. Ross, Phys. Lett. B **93** (1980) 313; C. J. Benesh and G. A. Miller, Phys. Lett. B **215** (1988) 381; R. P. Bickerstaff and J. T. Londergan, Phys. Rev. D **42** (1990) 3621; A. W. Schreiber, A. I. Signal and A. W. Thomas, Phys. Rev. D **44** (1991) 2653; H. Meyer and P. J. Mulders, Nucl. Phys. A **528** (1991) 589; T. Frederico and G. A. Miller, Phys. Rev. D **50** (1994) 210; C. M. Shakin and W. D. Sun, Phys. Rev. C **51** (1995) 2171; H. Weigel, L. P. Gamberg and H. Reinhardt, Phys. Lett. B **399** (1997) 287 [arXiv:hep-ph/9604295]; R. Jakob, P. J. Mulders and J. Rodrigues, Nucl. Phys. A **626** (1997) 937 [arXiv:hep-ph/9704335]; W. Bentz, T. Hama, T. Matsuki and K. Yazaki, Nucl. Phys. A **651** (1999) 143 [arXiv:hep-ph/9901377]; A. E. Dorokhov and L. Tomio, Phys. Rev. D **62** (2000) 014016; M. B. Hecht, C. D. Roberts and S. M. Schmidt, Phys. Rev. C **63** (2001) 025213 [arXiv:nucl-th/0008049]; M. Praszalowicz and A. Rostworowski, Phys. Rev. D **64** (2001) 074003 [arXiv:hep-ph/0105188]; E. Ruiz Arriola, arXiv:hep-ph/0107087.

[7] T. Shigetani, K. Suzuki and H. Toki, Phys. Lett. B **308** (1993) 383 [arXiv:hep-ph/9402286].

[8] R. M. Davidson and E. Ruiz Arriola, Phys. Lett. B **348** (1995) 163; H. Weigel, E. Ruiz Arriola and L. P. Gamberg, Nucl. Phys. B **560** (1999) 383 [arXiv:hep-ph/9905329].

[9] H. Weigel, E. Ruiz Arriola and L. P. Gamberg, Nucl. Phys. B **560** (1999) 383 [arXiv:hep-ph/9905329].

[10] V. N. Gribov and L. N. Lipatov, Yad. Fiz. **15** (1972) 781 [Sov. J. Nucl. Phys. **15** (1972) 438]; Yu. L. Dokshitzer, Sov. Phys. JETP **46** (1977) 641 [Zh. Eksp. Teor. Fiz. **73** (1977) 1216]; G. Altarelli and G. Parisi, Nucl. Phys. B **126** (1977) 298.

[11] J. F. Owens, Phys. Rev. D **30** (1984) 943.

[12] P. Aurenche, R. Baier, M. Fontannaz, M. N. Kienzle-Focacci and M. Werlen, Phys. Lett. B **233** (1989) 517.

[13] M. Glück, E. Reya and A. Vogt, Z. Phys. C **53** (1992) 651.

[14] M. Glück, E. Reya and I. Schienbein, Eur. Phys. J. C **10** (1999) 313 [arXiv:hep-ph/9903288].

[15] P. J. Sutton, A. D. Martin, R. G. Roberts and W. J. Stirling, Phys. Rev. D **45** (1992) 2349.

[16] Y. Nambu and G. Jona-Lasinio, Phys. Rev. **122** (1961) 345; Phys. Rev. **124** (1961) 246.

[17] M. Jaminon, R. Mendez Galain, G. Ripka and P. Stassart, Nucl. Phys. A **537** (1992) 418.

[18] C. Itzykson and J. B. Zuber, *Quantum Field Theory*, New York, U.S.A.: Mcgraw-hill (1980) 705 P. (International Series In Pure and Applied Physics).

[19] M. Klasen, J. Phys. G **28** (2002) 1091 [arXiv:hep-ph/0107011].

[20] G. E. Brown, M. Rho and W. Weise, Nucl. Phys. A **454** (1986) 669.